

Crystallization behaviour of poly(tetramethylene succinate)

Tadakazu Miyata^{a,*} and Toru Masuko^b

^aAdvanced Technology Research Laboratory, Oji Paper Co. Ltd., 1-10-6 Shinonome, Koto-ku, Tokyo 135, Japan

^bFaculty of Engineering, Yamagata University, 4-3-16, Jonan, Yonezawa, Yamagata 992, Japan

(Received 4 February 1997; revised 2 April 1997)

The bulk crystallization behaviour of poly(tetramethylene succinate) (PTMS) has been studied in terms of cooling rate and supercooling. The crystallinity of PTMS increased with decrease in cooling rate during the cooling process from the melt. The equilibrium melting point and the glass transition temperature of PTMS were found to be about 132°C and -38°C, respectively. The PTMS spherulites appeared to be negatively birefringent, and their linear growth rates were measured at various temperatures isothermally. The growth rate data obtained could be examined in terms of the kinetic theory of crystallization; thus the nucleation parameters of PTMS were explained quantitatively. © 1997 Elsevier Science Ltd. All rights reserved.

(Keywords: poly(tetramethylene succinate); crystallization kinetics; spherulite)

INTRODUCTION

Recently, aliphatic polyesters have received much attention regarding their biodegradability, particularly from an ecological point of view; this aspect has been studied extensively in order to replace some of the synthetic polymers that cause environmental problems due to their chemical stability. The mechanical properties and degradation rates of the polymers are associated with their morphology and crystallinity as well as their chemical structures. Therefore, results on the biodegradation of aliphatic polyesters obtained by individual researcher workers indicate small differences, even though specimens of similar chemical structure and molecular weight are examined.

Poly(tetramethylene succinate) (PTMS) is one of the interesting biodegradable synthetic polymers^{1,2}, and several publications concerned with investigations of PTMS in the solid state by X-ray diffraction (XRD) or electron microscopy³⁻⁶ have already appeared. Chatani *et al.*³ have reported that the crystal structure (α -form) of PTMS is monoclinic with unit cell dimensions $a = 0.521$ nm, $b = 0.914$ nm, $c = 1.094$ nm; $\beta = 124^\circ$; $P2_1/n-C_2h$ ⁵; the polymer chain might have a T₇GTG conformation. Using electron diffraction, Ihn *et al.*⁴ have recently reported similar values of the lattice constants to those of Chatani *et al.* Furthermore, Ichikawa *et al.*^{5,6} have proposed another crystal modification (β -form) which contains the T₁₀ helical chains of PTMS, and exists under strain.

Apart from these findings, Horii *et al.*⁷ have examined the molecular mobilities of PTMS in its amorphous region by ¹³C n.m.r. spectroscopy.

However, the bulk crystallization mechanism for PTMS has not been examined in detail until now. The relationship between structural features and crystallization (or annealing)

conditions in an isothermal or non-isothermal process is required from a fundamental point of view.

In the present study, we examine the crystallization characteristics of PTMS films under various thermal conditions with respect to their crystallinity and spherulite morphology.

EXPERIMENTAL

Materials

Commercial PTMS (Showa High Polymer Co., Ltd.) was used in this work. The PTMS pellets were dissolved in chloroform and then reprecipitated repeatedly in methanol. The purified polymer obtained was white and fibrous in appearance. Characterization data obtained by ¹H n.m.r. analysis, i.r. measurements and g.p.c. for the PTMS investigated are listed in Table 1.

Film specimens

A small amount of PTMS, sandwiched between two glass plates, was heated above its melting point (T_m) and then quenched in liquid nitrogen to form a film.

Using a d.s.c. apparatus described later, the PTMS films were crystallized isothermally at various temperatures for 60 min by cooling the samples quickly from 200°C in a nitrogen purge. These results gave us the equilibrium melting point of the PTMS. In the case of non-isothermal experiments, the samples were cooled at different rates from 200°C down to room temperature.

For the observations with an optical microscope, PTMS films about 10 μ m thick were cast by dropping 1 wt.% chloroform solution on to a glass plate in an air oven, followed by drying in a vacuum oven at room temperature.

D.s.c. measurements

The thermal properties of the PTMS films were characterized by use of a SEIKO DSC-200 calorimeter in

* To whom correspondence should be addressed

Table 1 Characteristics of the PTMS used in this work

Measurement method	Characteristic
I.r. absorption spectroscopy	Ester C=O, 1740 cm ⁻¹ Ester -O-, 1187 cm ⁻¹
¹ H n.m.r. spectrometry	1.71 ppm 2.63 ppm 4.11 ppm
G.p.c.	$\bar{M}_w = 1.14 \times 10^5$ $\bar{M}_w/\bar{M}_n = 3.1$

the range from -100 to 200°C at various heating (or cooling) rates in a nitrogen purge.

Optical microscopy

The thin-cast films were examined using an Olympus BH-2 polarizing microscope with a video camera system. A Linkam THM-600 hot stage device was also utilized in the range from 25 to 200°C above the T_m of PTMS.

For measuring the spherulite growth rates, we crystallized the PTMS thin-cast films at different temperatures isothermally after rapidly cooling the samples from 200°C. The *in situ* sizes of the spherulites were measured by use of a polarizing microscope with a hot stage device.

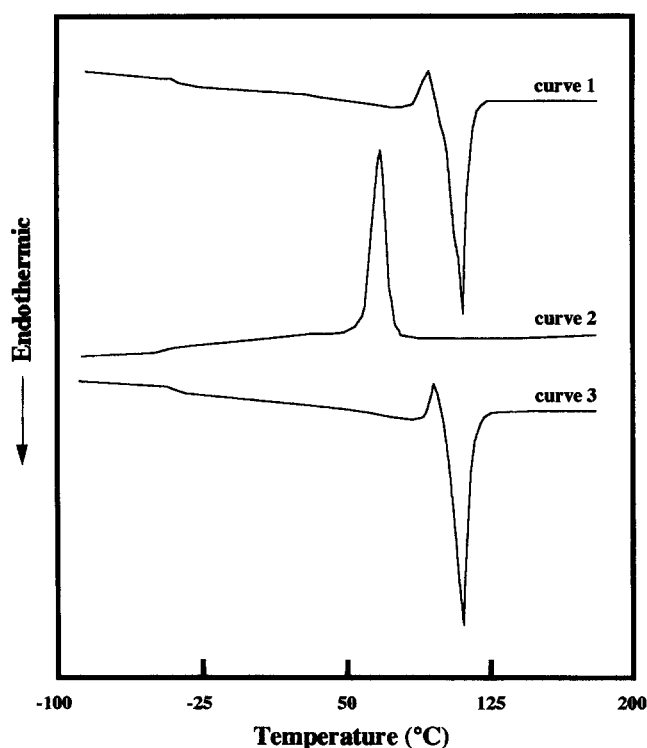
Density measurements

The density of the cast films was measured at 25°C using a flotation method employing aqueous CaBr₂ solution.

RESULTS AND DISCUSSION

Non-isothermal crystallization behaviour of the PTMS films

Figure 1 shows the d.s.c. heating and cooling curves of a melt-cast PTMS film at a rate of 20°C min⁻¹. The glass transition occurs at around -38°C. A single exothermic

**Figure 1** D.s.c. traces for the PTMS film in heating/cooling cycles

peak is located at 96°C, and an endothermic peak (T_m) appears at 110°C⁵ in the first-heating run (curve 1).

In order to examine the exothermic characteristics appearing in the d.s.c. trace, X-ray diffraction (XRD) measurements at elevated temperatures were made. The XRD profiles obtained in the range from 80 to 108°C indicated the same *d*-spacings of the PTMS film at room temperature. Therefore, the exothermic behaviour is related simply to the recrystallization of this polymer, independent of polymorphism.

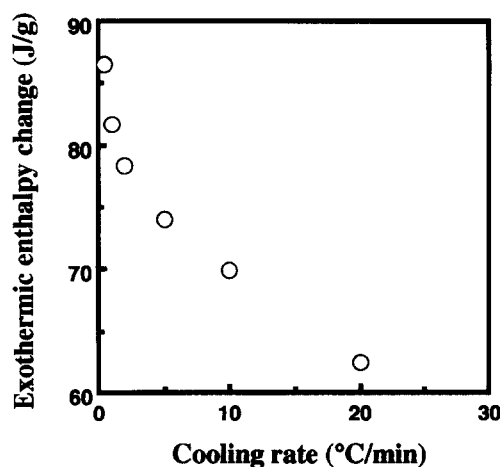
When the specimen was cooled from 200°C at 20°C min⁻¹, the exothermic crystallization peak and the glass transition temperature (T_g) are observed at 68°C and -40°C, respectively (curve 2). In the course of the second-heating run, a similarly shaped thermogram to curve 1 is observed (curve 3). After the heating/cooling cycle through T_m is repeated, the result for the first d.s.c. run is quite reproducible at the same heating/cooling rate.

Whenever the film specimens have been rapidly cooled from the isotropic melt at any rate higher than 20°C min⁻¹, they have crystallized rapidly. To clarify the crystallization behaviour of PTMS in the cooling process from the isotropic melt, the specimens were held in the d.s.c. pan at 200°C for 10 min, and then cooled to room temperature at various cooling rates.

Figure 2 shows plots of the exothermic enthalpy change (ΔH_{exo}) as a linear function of the cooling rate. The intrinsic value of ΔH_{exo} , obtained by extrapolating the cooling rate to 0°C min⁻¹ in Figure 2, is calculated to be about 110 J g⁻¹. Whenever the exothermic enthalpy change is 0, the cooling rate obviously becomes faster than 150°C min⁻¹, as seen from this relationship. Therefore, even if the PTMS films are cooled at any rate, the resultant films cannot become completely amorphous.

The density of the specimens increases with decrease in the cooling rate, as shown in Figure 3. This tendency resembles the relationship between the change in cooling rates and the exothermic enthalpy changes.

As shown in Figure 4, there exists a linear relationship between exothermic enthalpy change and density for the PTMS film. Since the density of the PTMS crystal (α -form) has the value 1.34 g cm⁻³⁴, the exothermic enthalpy of crystallization for a large crystal of infinite size is deduced to be 200 J g⁻¹ using this relationship. We can relate this value with the enthalpy of fusion. Furthermore, the 'amorphous density' of this polymer is estimated to be about 1.18 g cm⁻³.

**Figure 2** The exothermic enthalpy change as a function of the cooling rate

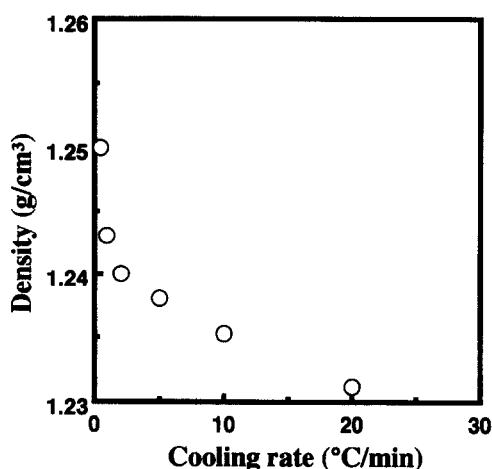


Figure 3 Changes in film density as a function of cooling rate from the isotropic melt

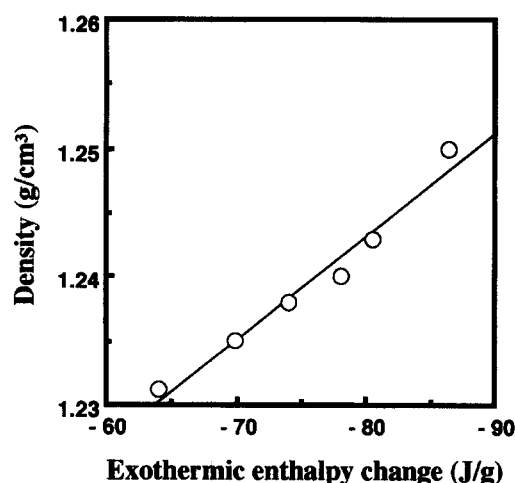


Figure 4 Relationship between exothermic enthalpy change and density for PTMS film specimens

As described earlier, when the exothermic enthalpy change is speculated as being 110 J g^{-1} for a cooling rate of 0°C min^{-1} , the maximum crystallinity of an annealed PTMS film is calculated to be 0.6. The crystallinity of a PTMS film crystallized at 90°C for 24 h is 0.6 from density measurements. Therefore, it seems difficult for the maximum crystallinity of the PTMS film to exceed a value of 0.6. As described above, the crystallinity of the PTMS film can be controlled effectively by changing the cooling rate, when the specimens are cooled from the melt.

Figure 5 shows optical micrographs of PTMS spherulites crystallized by cooling from 200°C (above the T_m) to room temperature at various rates. The size of the PTMS spherulite increases with decreasing cooling rates; at slower cooling rates (below 2°C min^{-1}) particularly, the PTMS film crystallizes effectively in association with the annealing treatment.

Isothermal crystallization characteristics of PTMS

Hoffman and Weeks⁸ have shown a relationship between T_m and the isothermal crystallization temperature, T_c

$$T_m = T_m^0 \left(1 - \frac{1}{2\beta}\right) + \frac{T_c}{2\beta} \quad (1)$$

where T_m^0 is the equilibrium melting point, and β is a

constant depending on the edge free surface energy of a crystalline polymer. Figure 6 shows the relationship between T_c and T_m for films crystallized under isothermal conditions. The extrapolation of T_m versus T_c to the line $T_m = T_c$ shows the value of T_m^0 to be 132°C (405 K).

The spherulites grown from the melt under isothermal conditions are negatively birefringent. The changes in the radius growth rates (G) of the PTMS spherulites were obtained as a linear function of crystallization time at all the temperatures investigated. The values of G in the limited range of T_c are shown in Figure 7. Measurements of the growth rate below 85°C were difficult since nucleation in the specimen occurred so rapidly. Figure 7 indicates that the G value decreases with increasing T_c . This behaviour resembles common features appearing in many synthetic polymers⁹.

In particular, spherulites with clear shapes are observed at low T_c (see Figure 8a). As the T_c is increased, the spherulites begin to show irregular shapes and coarse-grained structures are observed (Figure 8b). At high T_c , morphological changes from spherulitic to axialite-like texture are observed, especially for the case at 105°C (Figure 8c). However, we can hardly distinguish the two types of negative spherulite, as reported by Ihn *et al.*⁴.

These growth rate data have been examined in terms of the secondary nucleation theory¹⁰. The general expression for the growth rate of a linear polymer crystal with folded chains is given by

$$G = G_0 \exp\left[\frac{-U^*}{R(T_c - T_\infty)}\right] \exp\left(\frac{-Kg}{T_c \Delta T f}\right) \quad (2)$$

where Kg is the nucleation constant, ΔT is the supercooling $T_m^0 - T_c$, T_m^0 is the equilibrium melting point, f is the factor $2T_c/(T_m^0 + T_c)$, U^* is the activation energy for the transport of segments to the crystallization site, R is the gas constant, T_∞ is the hypothetical temperature where all motion associated with viscous flow ceases, and G_0 is the front factor. We apply the equation to our PTMS data shown in Figure 7.

Figure 9 presents plots of $\log G + U^*/2.303R(T - T_\infty)$ versus $1/T_c \Delta T f$, from which are obtained the value of Kg (from the slope) and $\log G_0$ (from the intercept). As the kinetic features are governed by the nucleation term, the results are relatively insensitive to the value of U^* . Here we have utilized the values of $U^* = 6300 \text{ J mol}^{-1}$ ($1500 \text{ cal mol}^{-1}$) and $T_\infty = T_g - 30$, since these values are recognized to be appropriate for a number of crystalline polymers¹⁰⁻¹². Under such an assumption, we obtained linear fits as shown in Figure 9. Along with the data used in this work, the results obtained from secondary nucleation analyses are listed in Table 2. There is no direct information on the

Table 2 Results of the secondary nucleation analysis

Quantity	Value	Source
Kg	0.551×10^5	—
$\sigma\sigma_c \text{ (J}^2 \text{ m}^{-4}\text{)}$	560×10^{-6}	—
<i>Parameters used in this analysis</i>		
$\Delta h_f \text{ (J m}^{-3}\text{)}$	268×10^6	This work
$T_m^0 \text{ (}^\circ\text{C)}$	132	This work
$d_{110} \text{ (m)}$	4.5×10^{-10}	Ref. 4
$T_g \text{ (}^\circ\text{C)}$	-38	This work
$T_\infty \text{ (}^\circ\text{C)}$	-68	$T_g - 30$
$U^* \text{ (J mol}^{-1}\text{)}$	6300	Ref. 9

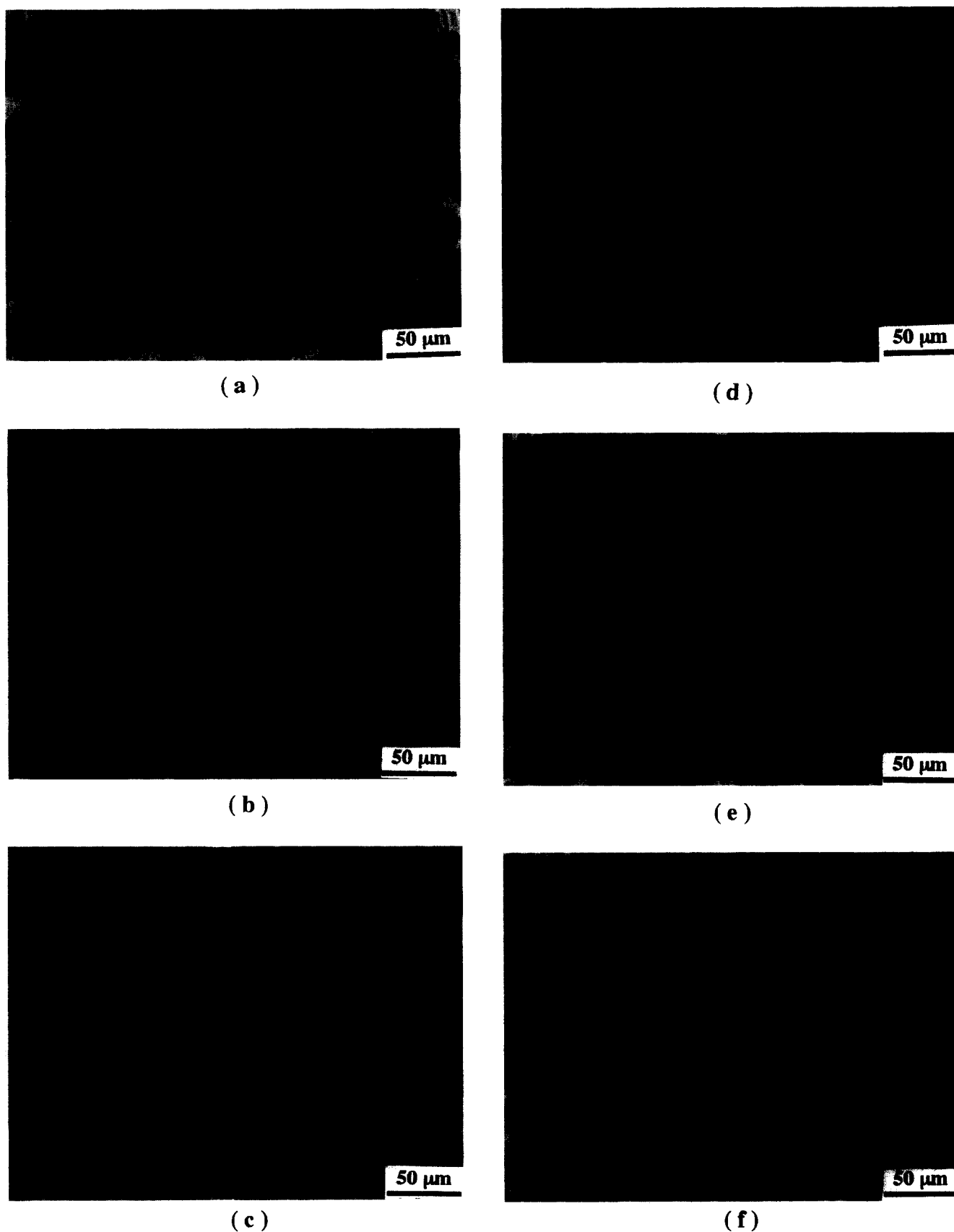


Figure 5 Optical micrographs of PTMS spherulites crystallized at various cooling rates from 200°C. (a) 0.5°C min⁻¹; (b) 1°C min⁻¹; (c) 2°C min⁻¹; (d) 5°C min⁻¹; (e) 10°C min⁻¹; (f) 20°C min⁻¹

growth front of a spherulite, because the lamellae structure of PTMS has not yet been established sufficiently. When a growth front is assumed to be the (110) plane in the present study, as in the case of high density polyethylene,

the layer thickness is calculated to be 0.45 nm for PTMS crystals. Accordingly, the values of K_g and the surface free energy $\sigma\sigma_c$ were obtained by assuming regime II growth¹⁰.

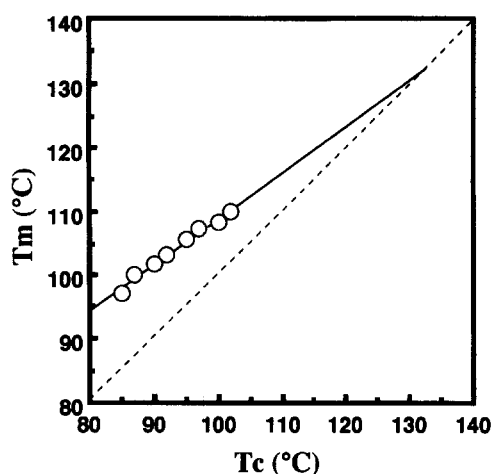


Figure 6 Changes in the T_m of PTMS as a function of the crystallization temperature, T_c . The extrapolation of the data to the line $T_m = T_c$ yields the

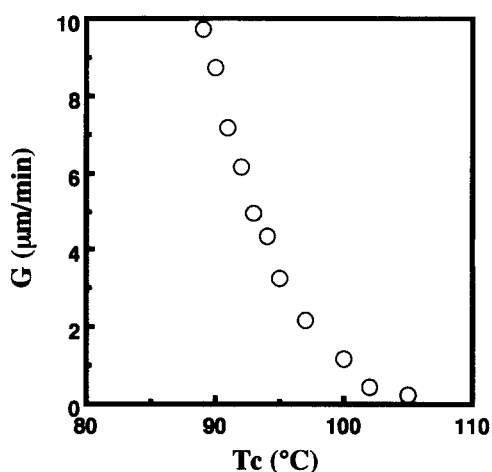


Figure 7 Radius growth rate G as a function of T_c

The nucleation parameter Kg is given by

$$Kg = \frac{2b\sigma\sigma_e T_m^0}{\Delta h_f k_B} \quad (3)$$

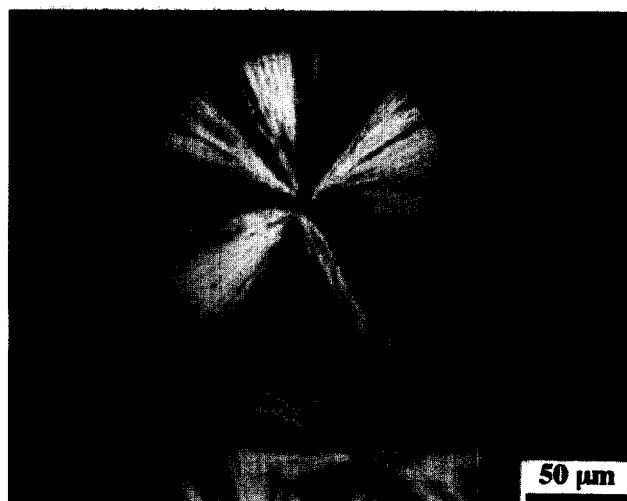
where b is the layer thickness, σ is the lateral surface energy, σ_e is the fold surface free energy, Δh_f is the heat of fusion per unit volume, and k_B is the Boltzmann constant. The value of $\sigma\sigma_e$ for PTMS is about $560 \times 10^{-6} \text{ J}^2 \text{ m}^{-4}$, approximately half of the value for polyethylene¹⁰.

Since axialite-like morphology is observed, as shown in Figure 8c, regime I would be applicable. Although attempts were made to analyze the growth rate data at the higher T_c , it was difficult to obtain enough sufficiently accurate data points for G for an acceptable secondary nucleation analysis.

A more detailed examination of the negatively birefringent spherulites of this polymer with respect to morphology and structure is necessary for obtaining more information concerning the mechanism and mode of spherulite growth in PTMS.

CONCLUSIONS

The crystallization characteristics of poly(tetramethylene succinate) (PTMS) have been studied by a d.s.c. method and optical microscopy.



(a)



(b)



(c)

Figure 8 Optical micrographs of (a) spherulites grown at 90°C, (b) irregularly shaped and coarse-grained spherulites grown at 100°C, and (c) axialites grown at 105°C

- (1) The crystallinity of PTMS depends closely on the cooling rate when the specimens are cooled from the isotropic melt.
- (2) Negatively birefringent PTMS spherulites are grown

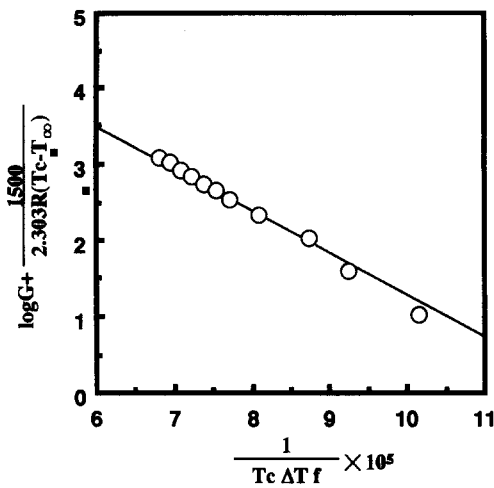


Figure 9 Changes in $\log G + U^*/2.303R(T_c - T_\infty)$ as a function of $1/T_c \Delta T f$

from the melt. The linear growth rate of the spherulites depends on the supercooling.

- (3) Surface free energy of the PTMS crystallite nucleus have been estimated from the growth rate data by application of the secondary nucleation theory.

ACKNOWLEDGEMENTS

The authors appreciate the contributions of Mr. Kazuo Sasaki of Yamagata University, who has carried out some parts of the work and arranged materials.

REFERENCES

1. Yokota, Y., Ishioka, R. and Watanabe, N., in Abstr. of the 3rd Int. Scientific Workshop on Biodegradable Plastics and Polymers, Osaka, 1993, p. 96.
2. Nishioka, M., Tuzuki, T., Wanajyo, Y., Oonami, F. and Horiuchi, T., in Abstr. of the 3rd Int. Scientific Workshop on Biodegradable Plastics and Polymers, Osaka, 1993, p. 97.
3. Chatani, Y., Hasegawa, R. and Tadokoro, H., *Polymer Prepr. Jpn.*, 1971, **20**, 420.
4. Ihn, K. J., Yoo, E. S. and Im, S. S., *Macromolecules*, 1995, **28**, 2460.
5. Ichikawa, Y., Suzuki, J., Washiyama, J., Moteki, Y., Noguchi, K. and Okuyama, K., *Polymer*, 1994, **35**, 3338.
6. Ichikawa, Y., Washiyama, J., Moteki, Y., Noguchi, K. and Okuyama, K., *Polym. J (Tokyo)*, 1995, **27**, 1230.
7. Horii, F., Hirai, A., Murayama, K., Kitamura, R. and Suzuki, T., *Macromolecules*, 1983, **16**, 273.
8. Hoffman, J. D. and Weeks, J. J., *J. Res. Natl. Bur. Stand.*, 1962, **66a**, 13.
9. Magill, J. H., *J. Appl. Phys.*, 1964, **35**, 3249.
10. Hoffman, J. D., Davis, G. T. and Lauritzen, J. I., *Treaties on Solid State Chemistry*, Vol. 3, ed. N. B. Hannay, Plenum, New York, 1976.
11. Vasanthakumari, R. and Pennings, A. J., *Polymer*, 1983, **24**, 175.
12. Phillips, P. J. and Rensch, G. J., *J. Polym. Sci., Part B*, 1989, **27**, 155.